DEVELOPMENT OF A ROBUST NUMERICAL MODEL USING CFD APPROACH TO ANALYSE THE FLOW CHARACTERISTIC INSIDE A CYCLONE SEPARATOR

By

KHONG JUN YONG

(120558)

Supervisor:

ASSOCIATE PROFESSOR DR FARZAD ISMAIL

June 2017

This dissertation is submitted to

Universiti Sains Malaysia

As a partial fulfilment of the requirement to graduate with honors degrees in

BACHELOR OF ENGINEERING (AEROSPACE ENGINEERING)

School of Aerospace Engineering

Engineering Campus

Universiti Sains Malaysia

DEVELOPMENT OF A ROBUST NUMERICAL MODEL USING CFD APPROACH TO ANALYSE THE FLOW CHARACTERISTIC INSIDE A CYCLONE SEPARATOR

ABSTRACT

Simulation using computational fluid dynamic techniques were performed intending to analyse the flow characteristic inside a cyclone separator in four different inlet velocities, $7\text{ms}^{-1}, 13ms^{-1}, 16ms^{-1}, and\ 22ms^{-1}$. The experimental data used in validation of simulations were obtained from the literature. Ideal y^{+} is controlled with the calculation of first layer thickness and grids verification is done. K-epsilon RNG and Reynolds Stress Models are used to simulate the model. Flow characteristic study is done in transient state with a developed robust numerical model. Profiles and contours show velocity magnitude vector, vorticity, static pressure, turbulent kinetic energy, and RMS of turbulent velocity fluctuation. RSM model is used results in less discrepancy in term of static pressure drop. The air flow inside the cyclone separator is highly turbulent and air flow behaviour is clearly observed.

PEMBANGUNAN MODEL BERANGKA TEGUH MENGGUNKAN PENDEKATAN CFD UNTUK MENANALISIS CIRI-CIRI ALIRAN DALAM PEMISAH SIKLON

ABSTRAK

Simulasi menggunakan teknik CFD telah dijalankan untuk menganalisis ciri-ciri aliran dalam pemisah siklon dalam empat halaju masuk yang berbeza, iaitu $7\text{ms}^{-1}, 13ms^{-1}, 16ms^{-1}, and\ 22ms^{-1}$. Data eksperimen yang digunakan dalam pengesahan simulasi telah diperolehi daripada kesusasteraan. Ideal y^{+} telah dikawal dengan pengiraan ketebalan lapisan pertama dan pengesahan grid telah dilakukan. K-epsilon RNG and Reynolds Stress Model telah digunakan untuk mensimulasikan model. Kajian ciri-ciri aliran telah dilakukan dalam keadaan fana dengan model yang tegap. Profil dan kountur menunjukkan halaju magnitude vector, kepusaran, tekanan static, tenaga kinetic bergelora, dan RMS untuk turan naik halaju bergelora. Model RSM digunakan kerana percanggahan dari segi kejatuhan tekanan static berkurang. Aliran udara dalam pemisah siklon adalah sangat bergelora dan kelakuan aliran udara boleh diperhatikan dengan jelas.

ACKNOWLEDGEMENTS

In the first place, I would like to offer my sincerest appreciation to my supervisor, Associate Professor Dr Farzad Ismail, who always support me with his patience and vast research experience throughout this study. Sometime, I felt dispirited along this research. However, I really appreciate his constant inspiration and encouragement that motivates me to complete this study. I am proud of his student having the opportunity to experience the real research progression such as critical thinking, consistency, and perseverance instead of spoon-fed.

Besides that, I am thankful to the post graduate students, Mr Chang Wei Shyang, Mr Vishal Singh, Mr Sivaraj Gopal Krishnan and Mr Neoh Soon Sien for always being by my side. Their comments and suggestions during every progress update solve my question and accelerate my study progression. In addition, they are always ready to support and give me their hands when necessary.

Finally, I would like to thank my pervious internship supervisor, Aldo Malvin for his recommendations based on his working experience in simulating of cyclone separator using CFD approach. He always leads me to think critically and solve my questions.

Thank you to everyone who helps me before that makes my final year project meaningful, successful, fruitful and experience unforgettable.

DECLARATION

This work has not previously been accepted in substance for any degree and is not being concurrently submitted in candidature for any degree.

_____

KHONG JUN YONG

Date:

STATEMENT 1

This thesis is the result of my own investigations, except where otherwise stated. Other sources are acknowledged by giving explicit references. Bibliography/references are appended.

_____

KHONG JUN YONG

Date:

STATEMENT 2

I hereby give consent for my thesis, if accepted, to be available for photocopying and for interlibrary loan, and for the title and summary to be made available to outside organizations.

_____

KHONG JUN YONG

Date:

TABLE OF CONTENTS

LIST OF TABLES

LIST OF FIGURES

LIST OF ABBREVIATIONS

WHO	World Health Organization
PM	Particulate Matter
CFD	Computational Fluid Dynamic
RANS	Reynolds Average Navier-Stokes
k-ε	K-epsilon
RNG	Re-Normalisation Group
RSM	Reynolds Stress Transport Models
RMS	Root Mean Square

NOMENCLATURE

$\mathbf{y^+}$	:	Dimensionless Wall Distance
$\mathbf{k}$	:	Turbulence Kinetic Energy $[m^2/s^2]$
$\overline{\boldsymbol{u}}^{\mathbf{2}}$	:	Fluctuating Velocity in Axial Direction $[m/s]$
$\overline{\boldsymbol{v}}^{\mathbf{2}}$	:	Fluctuating Velocity in Radial Direction $[m/s]$
$\overline{\boldsymbol{w}}^{\mathbf{2}}$	:	Fluctuating Velocity in Tangential Direction $[m/s]$
$\mathbf{D}_{\boldsymbol{b}}$	:	Body Diameter $[mm]$
$\mathbf{h}_{\boldsymbol{b}}$	:	Body Height $[mm]$
$\mathbf{D}_{\boldsymbol{vf}}$	:	Vortex Finder Diameter $[mm]$
$\mathbf{h}_{\boldsymbol{vf}}$	:	Vortex Finder Height $[mm]$
$\mathbf{h}_{\boldsymbol{c}}$	:	Conical Height $[mm]$
$\mathbf{D}_{\boldsymbol{ct}}$	:	Cone-tip Diameter $[mm]$
$\mathbf{b}_{\boldsymbol{i}}$	:	Inlet Width $[mm]$
$\mathbf{h}_{\boldsymbol{i}}$	:	Inlet Height $[mm]$
$\boldsymbol{Re}$	:	Reynolds Number
$\boldsymbol{\rho}$	:	Density of Air, $\rho = 1.225 kg/m^3$
$\boldsymbol{v_i}$	:	Inlet Velocity $[m/s]$
$\boldsymbol{\mu}$	:	Dynamic Viscosity of Air, $\mu = 1.983\times10^{-5}$Pas
$\mathbf{C_f}$	:	Skin Friction Coefficient
$\boldsymbol{T_w}$	:	Wall Shear Stress $[Pa]$
$\boldsymbol{U_*}$	:	Friction Velocity $[m/s]$
$\boldsymbol{y}$	:	First Layer Thickness$[m]$
$\boldsymbol{V}$	:	Kinematic Viscosity of Air $[m^2/s]$
RMS	:	Root Mean Square of Turbulent Velocity Fluctuation $[m/s]$
I	:	Turbulent Intensity [%]
U	:	Mean Velocity Magnitude $[m/s]$

CHAPTER 1

INTRODUCTION

1.1. General Overview

Air pollution has been one of the world's primary environmental policy concerns since the late 1970s and it is still an issue which gets a lot of attention nowadays. According to the air quality database in May 2016 by World Health Organization, 98% of cities in low-middle income countries and 56% of cities in high income countries do not meet WHO air quality guidelines. In short, air pollution control is imperative to govern or eliminate the emission of substances into the atmosphere.

Cyclone separators are one of the most frequently used control device nowadays that use principle of inertia to remove particulate matter (PM) or particulates from air, gas, or liquid stream without using filter separation. These devices are famous for their low capital and maintenance cost, simple construction, and relatively small space requirements.

Large scale cyclones are commonly used in sawmills to remove sawdust from the exacted air. This inspire the founder of the Dyson, James Dyson to develop household bagless vacuum cleaners. Besides that, cyclones are used in kitchen ventilation to separate grease from the exhaust air and oil refineries to separate oils and gases.

Cyclone separator is mainly divided into 4 parts, which are inlet part, body part, conical part, and outlet part as shown in Figure 1. Cyclone separators make use of swirl to separate out the particulates using rotational effects and gravity through vortex separation. Larger or denser particles have excess inertia and fail to follow the rotating stream end up with falling to the bottom of the cyclone after hitting the wall. Conical system in the cyclone designs increase the efficiency of the particles collected because Smaller particles can be separated when the rotational radius of the stream reduces.

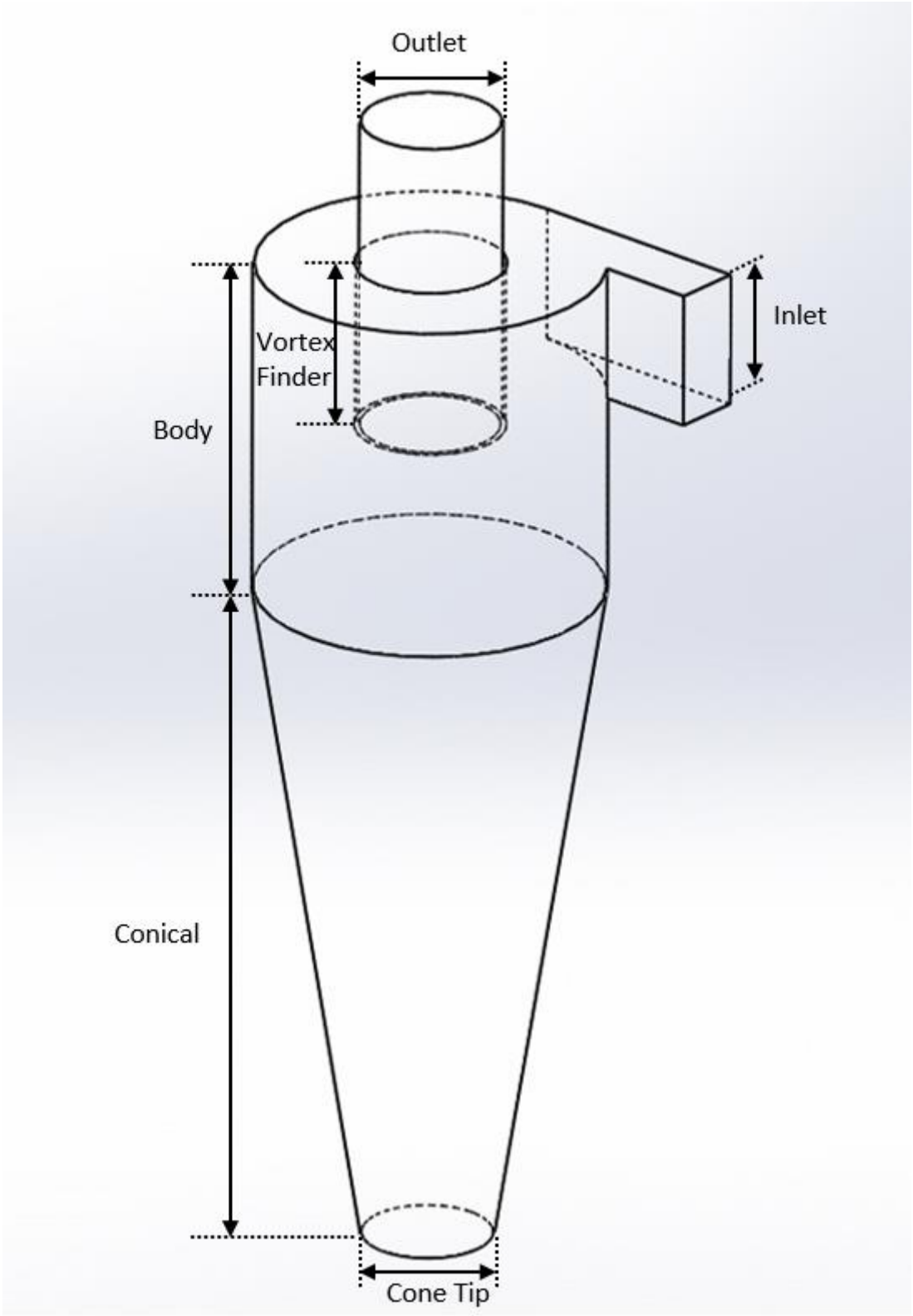

Figure 1: Structure of a Cyclone Separator

It is important to note that cyclones can vary drastically in their size. The size of the cyclone depends largely on how much flue gas must be filtered, and thus larger operations tend

to need larger cyclones. For example, several different models of one cyclone type can exist, and the sizes can range from a relatively small 1.2-1.5 meters tall (about 4-5 feet) to around 9 meters or about 30 feet (which is about as tall as a three-story building!). (1)

Plenty of studies have been done to investigate the effect of the geometry design to the performance of the cyclone separator. Slightly change in the dimension such as body height, conical height, and vortex finder changes the performance of cyclone separator in term of pressure drop and collection efficiency.

Cyclone separator collects dust using the effect of the swirling flow. When a dust-laden air stream enters a cyclone from the inlet, the flows go download in a spiral form. Particulates will be forced to the wall due to the inertial force and centrifugal force. Then, they will slide down to the bottom and the cone and collected. When the air stream spirals to the bottom, it flows in reserve direction and flow out the top of the cyclone. (2)

1.2. Motivation and problem statement

Cyclone separator has a very large potential market especially in controlling of air pollution from a large scale in industry such as sawmills to a small scale like household bagless vacuum cleaners. The flow development inside the cyclone is interesting and mystery. The cyclone does not need any motor or filter to swirl the flow and remove the dust. It is fully depending on the geometry design of the cyclone. Slightly change in design of the cyclone is more than enough to affect the performance significantly. Hence, a study on the flow behaviour inside the cyclone is conducted to understand the secret aerodynamic theory behind the working principles using Computational Fluid Dynamic approach.

In CFD, numerical model plays an important role to get a robust result. Meshing generation and boundary conditions in pre-processing and solution algorithm in solver are very imperative so that consistent results can be obtained in post-processing. Hence, validation of stimulation

results become very important because CFD will still give results with any data input without checking the reliability and sustainability of the numerical model. In this study, experimental result from the literature (3) is used to validate the reliability of the simulation results and determine the robustness of the numerical model.

1.3. Objective of Research

This study, "Development of a Robust Numerical Model using CFD approach to Analyse the Flow Characteristic inside a Cyclone Separator", is divided into two scopes.

The first scope of this study aims to develop a robust numerical model so that the results obtained have high reliability and consistent.

On the other hand, the second scope of this study is to study the flow behaviour inside the cyclone separator.

1.4. Thesis Layout

This thesis includes 5 chapters. Chapter 1 introduce the function of cyclone separator in term of pollution control and its fundamental working principle. In addition, the objective of this research is stated clearly with two primary scopes.

Chapter 2 illustrates the research have been done by the formers and emphasis on the pressure drop in the cyclone separator. Besides that, the study of grids verification and turbulence model validation by the formers are mentioned too.

Chapter 3 demonstrates the methodology of first scope, CFD working process in pre-processing such as mesh generation and boundary conditions. Grids selection is demonstrated with first layer thickness identification and skewness checking. Flow behaviour identification, which is the second scope of this study is identified in term of few parameters in term of quantitative and qualitative results.

Chapter 4 shows the results in developing of robust numerical model. Besides that, flow behaviour insides the cyclone separator is presented qualitatively and quantitatively. The key parameters that used in this flow characteristics investigation are velocity vector, RMS of turbulent velocity fluctuation, strength of vortices, and turbulent kinetic energy.

Chapter 5 concludes the outcome of this research. Further investigation is suggested to improve the observation of flow behaviour inside the cyclone separator.

CHAPTER 2

LITERATURE REVIEW

2.1. Design Improvement

In the past few decades, a great number of research has been dedicated to design and performance characteristics of cyclone separators. Basically, the main objective of the research is on cyclone inlet design, the vortex finder design, and the barrel of the cyclone. There is some most popular literature about the effective cyclone designs such as (4), (5), and (6). (7)

The most significant performance variables of cyclone separators are collection efficiency and pressure drop. Pressure drop is estimated as inlet and outlet losses combined with the loss of static head in the vortex (8) and cyclone inner friction surface (9).

2.2. Pressure Drop

Cyclone pressure drop fundamentally depends on the design of cyclone geometry, roughness of surface and operating conditions such as inlet velocity and gas temperature. Pressure drop can be divided into two parts, which are local losses and frictional losses in the cyclone body. Performance of cyclone separator can be identified by pressure drop. High pressure drop across the cyclone separator represents high dust collection efficiency. (10) Static pressure is commonly used to validate the simulation results because it can be obtained easily in experiment. Helicity and vorticity insides the flow losses energy too results in loss of static pressure. Hence, measurement of pressure drop is an alternative way to verify the flow as well as validate the numerical solution.

2.3. Grids Verification

To analyse fluid flows using the partial differential equations, flow domains must be split into smaller subdomains made up of geometric primitives, known as elements or cells. Collection of all elements or cells is called a mesh or a grid. (11) Meshing is very important because the

governing equations are discretized and solved inside these elements or cells. The solution is highly dependent on the quality of mesh as continuity of solution will be across the common interfaces between subdomains.

2.3.1 Dimensionless Wall Distance y^+

Boundary layer is a thin layer of fluid near the surface due to the shear stress and friction drag. Boundary layer is caused by viscous flow and dissipative effect due to friction, thermal conduction, or mass diffusion. (12) The flow inside cyclone separator has high Reynolds numbers results in turbulent boundary layer occurs. Steamwise velocity inside the turbulent boundary layer is characterized by unsteady swirling flows. Hence, equation solving in boundary layers near the wall become very important to get a precise result especially in turbulence model.

Dimensionless wall distance, y^+ is used to define how coarse or fine a mesh is for a flow pattern by determining the proper size of the cells near the domain walls. y^+can be estimated by calculating the first layer thickness from the wall using the free-stream velocity and gas data. Desired y^+ value can be set by estimating the wall distance to get the height of the boundary layer. Value of y^+ close to the lower bound, which is 30 are the most desirable for wall functions while, $y^+ \approx 1$ are the most desirable for near-wall modelling. (13)

2.3.2 Mesh Quality

The quality of the mesh can be identified based on the skewness of mesh. Skewness of mesh is one of the fatal features that determines the quality of mesh. It is defined on the geometrical orientation of a mesh and measured as difference from the ideal mesh cell. Skewness measure the percentage of the generated mesh differs from the ideal mesh cell. Skewness is calculated by measuring the angle between the normal vector of a face with the line joining the geometrical centre. (14) The maximum possible value then divides the resulting value and the

skewness ranged from 0 to 1. The lower the skewness, the better the mesh quality according to the Figure 2.

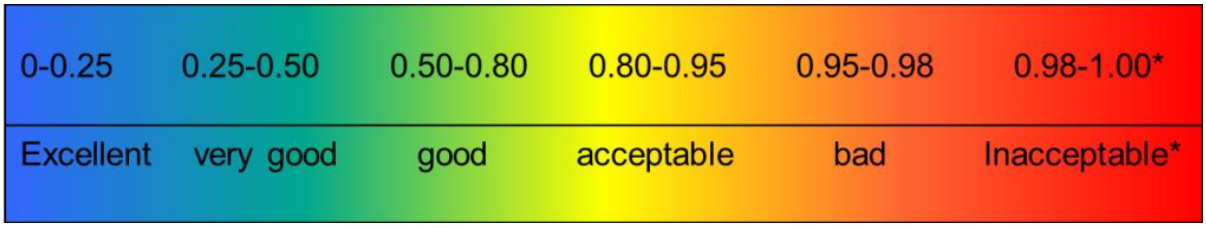

Figure 2: Skewness Quality Value, according to (15)

2.4. Turbulence Model Validation

Almost all engineering applications are turbulent. Hence, most CFD simulations need turbulence model to solve and get reliable results. In other words, selection of turbulence model is very important because it will highly affect the simulation results. (16)

Bradshaw. Et. Al. concluded that no current Reynolds Average Navier-Stokes (RANS) turbulence model can predict the whole range of complex turbulent flows to worthwhile engineering accuracy. Besides that, RANS model will give approximately 15% discrepancy. (17) Hence, selection of turbulence model becomes more vital to obtain high reliability results.

Validation is the process of determining the degree to which a model is an accurate representation of the real world from the perspective of the intended uses of model. Validation of results become very important especially in CFD simulation to ensure high accuracy and reliable results. (18) Since it is impossible to validate the entire CFD code, validation of a model or simulation using experimental data is frequently used to identify and quantify error and uncertainty through comparison.

Bradshaw. Et. Al. uses k-ε, k-ε RNG and RSM turbulence model to solve turbulent swirling flow in a cyclone separator. (19) Hoekstra concludes that both k-ε and k-ε RNG turbulence model are unsuitable for cyclonic flow due to the unrealistic distribution of axial and tangential

velocities predicted. RSM turbulence model is the most suitable and has the most reasonable agreement with experimental data even though discrepancies are still existing. (20)

2.5. Flow Study in Transient State Simulation

When the fluid undergoes irregular fluctuations, it is known as turbulence flow. The speed of the fluid inside the turbulent flow is continuously changing in both magnitude and direction. Turbulence can be observed as irregular swirls of motions, known as eddies. (21)

Transient state simulation is a process that variables change over time. There are some variables and higher order terms that are dealing with time can be only obtained from transient state simulation. Steady state simulation ignores all these term as they do not affect the steady state results. Hence, steady state simulation has an easier convergence and takes short time to solve compared to transient simulation because there are less terms to model.

If an unsteady flow were simulation in a steady state, the results will be poor or less accurate. Hence, transient simulation is necessary to study the flow behaviour inside a cyclone separator because it involves strong swirling flow and the flow is highly turbulence. Most importantly, turbulence may change in time.

2.5.1 Strength of Vortices

The vorticity is a scalar which is equal to the curl of the velocity. It is twice the angular velocity whereas angular velocity expresses the amount of rotation and distortion in the velocity field. Besides that, rotation of flow can be identified based on the angular velocity.

Vorticity is one of the most powerful quantities in theoretical aerodynamics especially in viscous flow. Generally, viscous flows are rotational and the strength of vorticity could be identified to determine the magnitude of rotational flow.

2.5.2 Turbulent Kinetic Energy

Turbulent kinetic energy is the mean kinetic energy per unit mass associated with eddies in turbulent flow. It is a measure of turbulence intensity and can be characterised by measured RMS velocity fluctuations, shown in Equation (1). From the turbulent kinetic energy, the mean of the turbulence normal stresses can be quantified.

$$k = \frac{1}{2}(\overline{u}^2 + \overline{v}^2 + \overline{w}^2) \quad (1)$$

2.5.3 Root Mean Square of Turbulence Velocity Fluctuation

Turbulent velocity fluctuation is due to the presence of small coherence structure such as vortices within the flow generated by the large-scale flow instabilities. RMS is the square root of arithmetic mean of the squares of a set of values. It is frequently used to measure the typical magnitude of the values regardless of their sign. The turbulence velocity fluctuation is manipulated by the vorticity of the small scale turbulent fluctuation, which is influenced by the vorticity of the mean boundary layer.

CHAPTER 3

METHODOLOGY

3.1. Computational Domain

The scale of the cyclone separator design from (3) is reproduced in the SOLIDWORKS 2016 x64 Edition and exported to ANSYS Workbench 16.1.

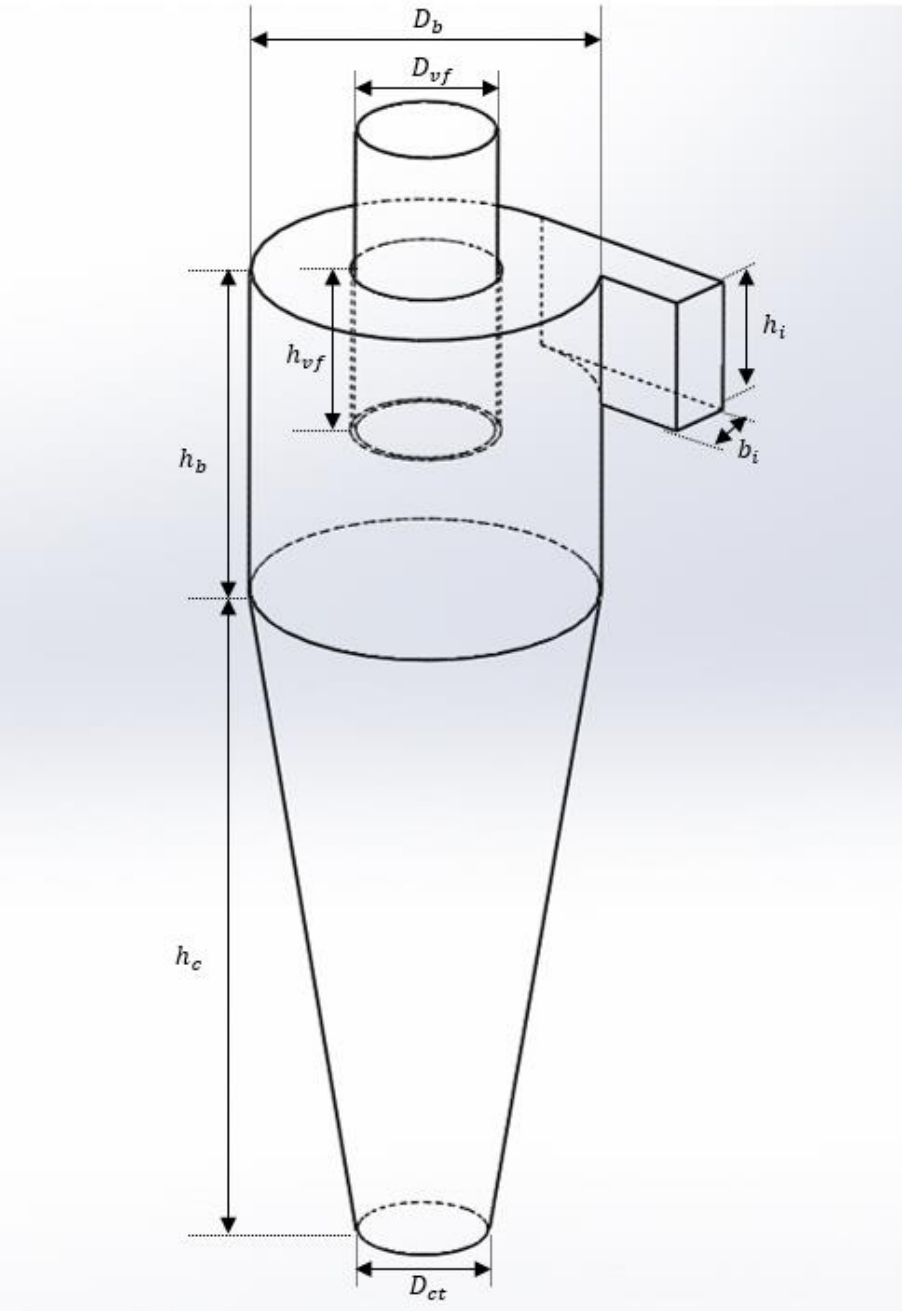

Figure 3: Dimensions of Cyclone Separator Reproduced from (3)

Table 1: Dimensions of Cyclone Separator Reproduced from (3)

Cyclone Geometry	Notations	Dimension (mm)
Body Diameter	D_b	290
Body Height	h_b	290
Vortex Finder Diameter	D_{vf}	116
Vortex Finder Height	h_{vf}	145
Conical Height	h_c	580
Cone-tip Diameter	D_{ct}	109
Inlet Width	b_i	58
Inlet Height	h_i	116

In addition, the whole cyclone separator is set to be fluid. Besides that, the experimental results are exported using WebPlotDigitizer Version 3.11 to validate the simulation results and determine the robustness of the numerical model shown in Table 2. Static pressure drop is obtained by getting the difference in static pressure between the inlet and outlet of the cyclone separator.

Table 2: Experimental Results exported from the (3)

Inlet Velocity (ms^{-1})	Static Pressure Drop (Pa)
9.95	238.5
11.78	340.3
13.56	462.1
15.28	614.5
17.15	787.0
18.43	923.3

3.2. Meshing

Firstly, the boundary condition is set as shown in Figure 4. The inlet boundary condition is set as velocity inlet and the outlet boundary condition is set as pressure-outlet. The remaining surfaces of the cyclone are set as stationary no-slip walls.

Besides that, a vertical plane across the centreline of the cyclone and a horizontal plane, 290mm from the tip of the body were built for the further study in the transient simulation.

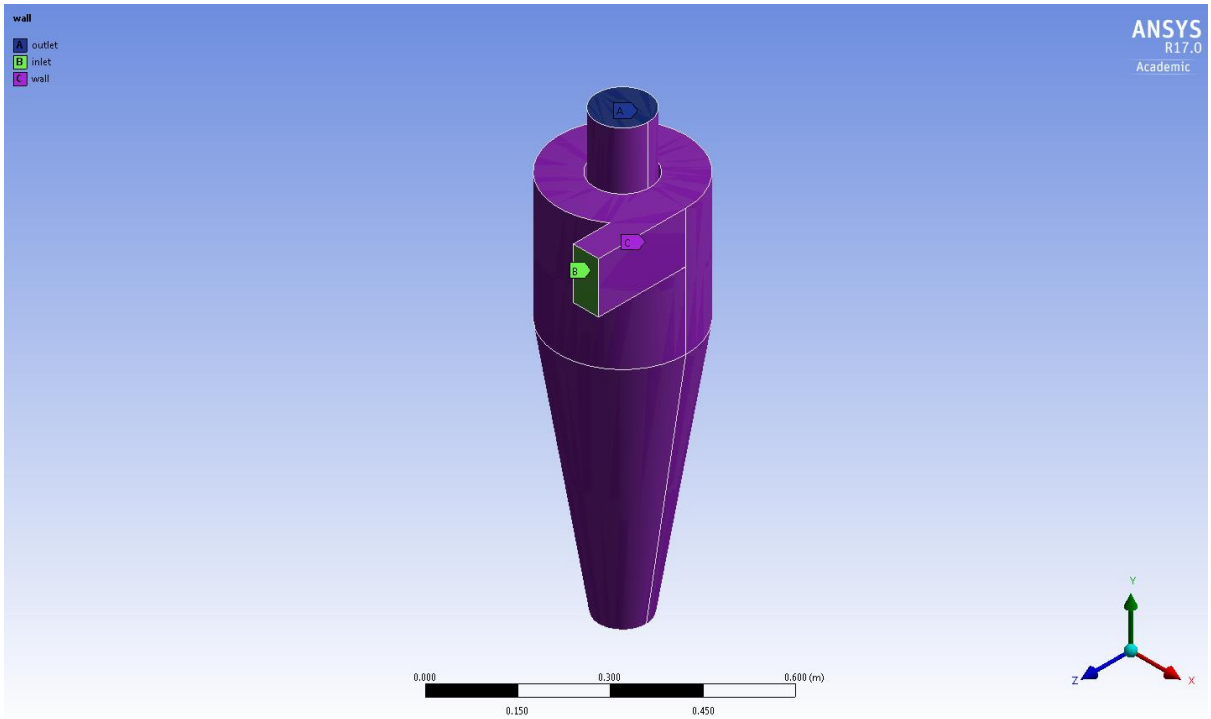

Figure 4: Boundary Conditions of the Cyclone

3.2.1 First Layer Thickness Identification

Wall y^+ value plays an important role to get a robust result and it can be controlled by the first layer thickness, y in inflation method. However, first layer thickness will change with different inlet velocity as it is a function of Reynolds Number and it changes with velocity.

Different Re were calculated with the inlet velocity provided from the (3) using Equation (2). Then, C_f, T_w, and U_* were calculated using Equation (3), Equation (4) and Equation (5) respectively. Lastly, y is calculated with friction velocity and ideal y^+ value of 1 using Equation (6). The results are shown in Table 3.

$$Reynolds\ Number, Re = \frac{\rho v_i D_b}{\mu} \times 1000 \quad (2)$$

$$Skin\ Friction\ Coefficient, C_f = (2\log RE - 0.65)^{-2.3} \text{ for } Re < 10^9 \quad (3)$$

$$Wall\ Shear\ Stress, T_w = C_f \times \frac{1}{2}\rho\mu^2 \quad (4)$$

$$Friction\ Velocity, U_* = \sqrt{\frac{T_w}{\rho}} \quad (5)$$

$$First\ Layer\ Thickness, y = \frac{y^+ V}{U_*} \quad (6)$$

$$\mathrm{V} = \frac{\mu}{\rho} \quad (7)$$

Table 3: First Layer Thickness Calculation Results

Inlet Velocity (ms^{-1})	9.95	11.78	13.56	15.28	17.15	18.43
Re	178252	211036	242924	273738	307238	330169
C_f	5.19E-03	5.01E-03	4.88E-03	4.76E-03	4.66E-03	4.59E-03
T_w	0.3145	0.4261	0.5491	0.6810	0.8389	0.9554
U_*	0.5067	0.5898	0.6695	0.7456	0.8275	0.8831
y (mm)	0.05147	0.03799	0.02948	0.02377	0.01930	0.01694

Thinnest first layer thickness value, 0.01694mm is used for the inflation method to make sure all different mesh have good wall y^+ value for all different inlet velocity.

3.2.2 Grids Selection

Three methods were used during meshing which are faces sizing on the inlet and outlet, faces sizing on the walls and inflation method on all the walls. Constant element size is used for the faces sizing on inlet and outlet and a growth rate of 1.2 with 30 inflation layers and first layer thickness of 0.01694mm were set for all mesh. Element size of the faces sizing on the walls is manipulated and four different mesh were developed.

Table 4: Mesh Results of 4 Different Mesh

Mesh	Faces Sizing		Inflation Method			Mesh Number
	Elements Size on Walls (m)	Element Size on Inlet & Outlet (m)	Growth Rate	Inflation Layers	First Layer Thickness(mm)	
Very Coarse	0.020	0.010	1.2	30	0.01694	184,196
Coarse	0.016					271,401
Intermediate	0.012					467,527
Fine	0.010					683,272

3.2.3 Mesh Quality

Skewness of mesh is one of the fatal features that determines the quality of mesh. It is defined on the geometrical orientation of a mesh and measured as difference from the ideal mesh cell.

Based on the Table 5, average skewness decreases with the number of mesh. According to the skewness quality value (15) shown in Figure 2, the maximum skewness for very coarse mesh is bad while the maximum skewness for the remaining mesh are acceptable. Basically, all meshes are considered as very good with the average skewness ranged from 0.3022 to 0.2421.

Table 5: Skewness Quality of the Mesh

Mesh	Skewness		
	Average	Minimum	Maximum
Very Coarse	0.3022	0.0014310	0.9722
Coarse	0.2776	0.0008842	0.9485
Intermediate	0.2519	0.0004686	0.9459
Fine	0.2421	0.0005677	0.9464

Simulations were run with different mesh at the lowest inlet velocity, 9.95ms^{-1} in steady state. K-epsilon (k-ε) RNG turbulence model is used for the grid selection simulation. Wall y^+ value is observed to make sure the average y^+ on the wall is within the ideal y^+ value, which is 1. Next, static pressure drop is measured from different mesh and the most effective grid is selected based on the results analysis. The best mesh will be brought to further study.

3.2.4 Wall y Plus Value

Table 6: y^+ on the Walls of Different Mesh

Mesh	y^+ on Walls		
	Average	Minimum	Maximum
Very Coarse	0.8195	0.05397	1.968
Coarse	0.8317	0.06495	1.998
Intermediate	0.8478	0.06575	2.023
Fine	0.8772	0.08145	2.097

Table 6 shows the y^+ on the walls of all mesh. The y^+ increases with the number of mesh. The average y^+ for all meshes are still less than ideal y^+, which is excellent even though the maximum y^+ are around 2. In short, the grids near to the walls are fine enough to solve the boundary layers.

3.3 Turbulence Model Validation

Viscous and incompressible fluid flow is also known as Navier-Stokes equations after Claude Louis Marie Henri Navier and George Gabriel Stokes, can be expressed as:

$$\nabla . \mathrm{u} = 0 \tag{8}$$

$$\rho \frac{\mathrm{Du}}{\mathrm{Dt}} = -\nabla \mathrm{p} + \mu \Delta u + \mathrm{F_B} \tag{9}$$

$\nabla .$ is the divergence operator, u is the velocity vector, ρ is the density of fluid, $\frac{\mathrm{Du}}{\mathrm{Dt}}$ is the acceleration of fluid, ∇ is the gradient operator, p is the fluid pressure, μ is the dynamic viscosity, and $\mathrm{F_B}$ is the body force.

Equation (8) is the conservation of mass in the context of constant-density flow while Equation (9) is the Newton's second law of motion applied to a fluid parcel. (22) The left-hand side is the product of the acceleration and density, while the right-hand side is the sum of forces acting on the fluid element.

In Reynolds-averaged, the solution variables in the instantaneous Navier-Stokes equations are decayed in to mean and fluctuating components such as time-averaged and fluctuating velocity.

For the velocity components:

$$\mathrm{u_i} = \overline{u_\imath} + u_i' \tag{10}$$

For the scalar quantities such as pressure, energy, or species concentration:

$$\emptyset_\mathrm{i} = \overline{\emptyset}_\imath + \emptyset_\mathrm{i}' \tag{11}$$

When the expressions of this form for the flow variables are substitute into the instantaneous continuity and momentum equations, written in Cartesian tensor form as:

$$\frac{\delta \rho}{\delta t} + \frac{\delta}{\delta x_i}(\rho u_i) = 0 \qquad (12)$$

$$\frac{\delta}{\delta t}(\rho u_i) + \frac{\delta}{\delta x_i}(\rho u_i u_j) = -\frac{\delta \rho}{\delta x_i} + \frac{\delta}{\delta x_i}\left(u\left(\frac{\delta u_i}{\delta x_j} + \frac{\delta u_j}{\delta x_i} - \frac{2}{3}\delta_{ij}\frac{\delta u_l}{\delta x_l}\right)\right) + \frac{\delta}{\delta x_j}(-\rho u_i' u_j') \qquad (13)$$

Equation (12) and Equation (13) are known as Reynolds-averaged Navier-Stokes equations. Basically, they have similar form as the instantaneous Navier-Stokes equations with time-averaged velocities and other solution variables. RANS equations represent transport equations for the mean flow quantities only. Two turbulence models from RANS models were used in turbulence model validation which are K-epsilon and RSM turbulence model.

K-epsilon (k-ε) turbulence model focuses on the turbulent kinetic energy, k, and the rate of dissipation of the turbulent energy, ε. K-epsilon (k-ε) RNG has additional term in dissipation equation for interaction between turbulence dissipation and mean shear stress. It includes the effect or swirl on turbulence and hence it is suitable for high streamline curvature and strain rate. The turbulent kinetic energy and the rate of dissipation of the turbulent energy of K-epsilon (k-ε) RNG can be expressed in Equation(14) and Equation(15) respectively.

$$\rho U_i \frac{\delta k}{\delta x_i} = \mu_t S^2 + \frac{\delta}{\delta x_i}\left(\alpha_k \mu_{eff} \frac{\delta k}{\delta x_i}\right) - \rho\varepsilon \qquad (14)$$

$$\rho U_i \frac{\delta \varepsilon}{\delta x_i} = C_{1\varepsilon}\left(\frac{\varepsilon}{k}\right)\mu_t S^2 + \frac{\delta}{\delta x_i}\left(\alpha_\varepsilon \mu_{eff} \frac{\delta \varepsilon}{\delta x_i}\right) - \rho C_{2\varepsilon}\left(\frac{\varepsilon^2}{k}\right) - R \qquad (15)$$

$\rho U_i \frac{\delta k}{\delta x_i}$ and $\rho U_i \frac{\delta \varepsilon}{\delta x_i}$ are convection transport, $\mu_t S^2$ and $C_{1\varepsilon}\left(\frac{\varepsilon}{k}\right)\mu_t S^2$ are the generation terms, $\frac{\delta}{\delta x_i}\left(\alpha_k \mu_{eff} \frac{\delta k}{\delta x_i}\right)$ and $\frac{\delta}{\delta x_i}\left(\alpha_\varepsilon \mu_{eff} \frac{\delta \varepsilon}{\delta x_i}\right)$ are the diffusion terms, $\rho\varepsilon$ is the dissipation term, $\rho C_{2\varepsilon}\left(\frac{\varepsilon^2}{k}\right)$ is the destruction term, and the R is an additional term related to mean strain and turbulence quantities in k-epsilon (k-ε) RNG.

Reynolds stresses in k-epsilon turbulence model can be calculated in Equation (16). μ_t is the turbulent viscosity that can be calculated from Equation (17).

$$-\rho\overline{u_i u_j} = \mu_t\left(\frac{\delta U_i}{\delta x_i} + \frac{\delta U_j}{\delta x_i}\right) - \frac{2}{3}\rho k\delta_{ij} \quad (16)$$

$$\mu_t = C_\mu \frac{k^2}{\varepsilon} \quad (17)$$

RSM closes the RANS equations by solving extra transport equations for six independent Reynolds stresses. RSM is suitable for predicting complex flows such as streamline curvature, swirl, rotation, and high strain rates. The exact equation for the transport of the Reynolds stress, $R_{ij}$is expressed in Equation (18):

$$\frac{\delta}{\delta t}\left(\rho\overline{u_i' u_j'}\right) + C_{ij} = P_{ij} + D_{ij} - \varepsilon_{ij} + F_{ij} + \emptyset_{ij} + D_{T,ij} + G_{ij} \quad (18)$$

$$\text{Local Time Derivative} = \frac{\delta}{\delta t}\left(\rho\overline{u_i' u_j'}\right) \quad (19)$$

$$Convection, C_{ij} = \frac{\delta}{\delta x_k}\left(\rho u_k\overline{u_i' u_j'}\right) \quad (20)$$

$$StressProduction\ , P_{ij} = -\rho\left(\overline{u_i' u_k'}\frac{\delta u_j}{\delta x_k} + \overline{u_j' u_k'}\frac{\delta u_i}{\delta x_k}\right) \quad (21)$$

$$Transport\ by\ Diffusion, D_{ij} = -\frac{\delta}{\delta x_k}\left(\rho\overline{u_i' u_j' u_k'} + p'\left(\overline{\delta_{jk}u_i' + \delta_{ik}u_j'}\right)\right) \quad (22)$$

$$\text{Rotation Transport}, F_{ij} = -2\rho\Omega_k\left(\overline{u_j' u_m'}\epsilon_{mik} + \overline{u_i' u_m'}\epsilon_{mjk}\right) \quad (23)$$

$$\text{Rate of Dissipation}, \varepsilon_{ij} = \overline{2\mu\frac{\delta u_i'}{\delta x_k}\frac{\delta u_j'}{\delta x_k}} \quad (24)$$

$$\text{Pressure} - \text{Strain}, \emptyset_{ij} = \overline{p\left(\frac{\delta u_i'}{\delta x_j} + \frac{\delta u_j'}{\delta x_i}\right)} \quad (25)$$

$$Molecular\ Diffusion, D_{T,ij} = \frac{\delta}{\delta x_k}\left(\mu \frac{\delta}{\delta x_k}\left(\mathrm{u_i}' u_j'\right)\right) \quad (26)$$

$$Buoyancy\ Production, G_{ij} = -\rho\beta\left(g_i \overline{u_j'\theta} + g_j \overline{u_i'\theta}\right) \quad (27)$$

However, ε_{ij}, $\emptyset_{ij}$, $D_{T,ij}$,and G_{ij} need to be modeled to close the equations. The fidelity of the RSM depends on the accuracy of the models for the turbulent transport, the pressure strain-correlation, and the dissipations terms. (23) k-ε turbulence model involves two equations which are calculation of k and ε. The Reynold stress must be calculated with another equation, shown in Equation (16). On the other hand, RSM turbulence model with seven equations involve the calculation of the individual Reynolds stresses, using differential transport equations shown in Equation (18).

Both RANS turbulence models are suitable for high swirling flow and high streamline curvature. Hence, K-epsilon (k-ε) RNG turbulence model and Reynolds Stress Model (RSM) were run at the same inlet velocity, which is $9.95\mathrm{ms}^{-1}$ to validate the most suitable turbulence model.

3.4 Flow Study in Transient State

2 inlet velocities within the working operation of the cyclone and another two out of working operation, based on the (3) were selected to study the flow in transient state. Hence, 4 different inlet velocities, which are 7 ms^{-1}, 13 ms^{-1}, 16 ms^{-1}, and 22 ms^{-1} were used to study the flow behaviour in transient state. Time step of 0.0005s with 2000 number of time step are selected for the transient state study. Data sampling of every interval is selected for time statistics.

Static pressure drop is measured to identify the performance and efficiency of the cyclone separator. Besides that, turbulent parameters such as turbulent kinetic energy, RMS of turbulent

velocity fluctuation and vorticity are observed at different inlet velocity. The radial profile of turbulent kinetic energy is plotted by getting the average turbulent kinetic energy in consistent interval of radial position.

3.4.1 Root Mean Square of Turbulent Velocity Fluctuation

Average RMS of turbulent velocity fluctuation is calculated to study the relationship between the magnitude of turbulent velocity fluctuation and inlet velocity, by using Equation (28).

$$RMS = \mathrm{I} \times \mathrm{U} \tag{28}$$

CHAPTER 4

RESULTS AND DISCUSSION

4.1. Grid Verification

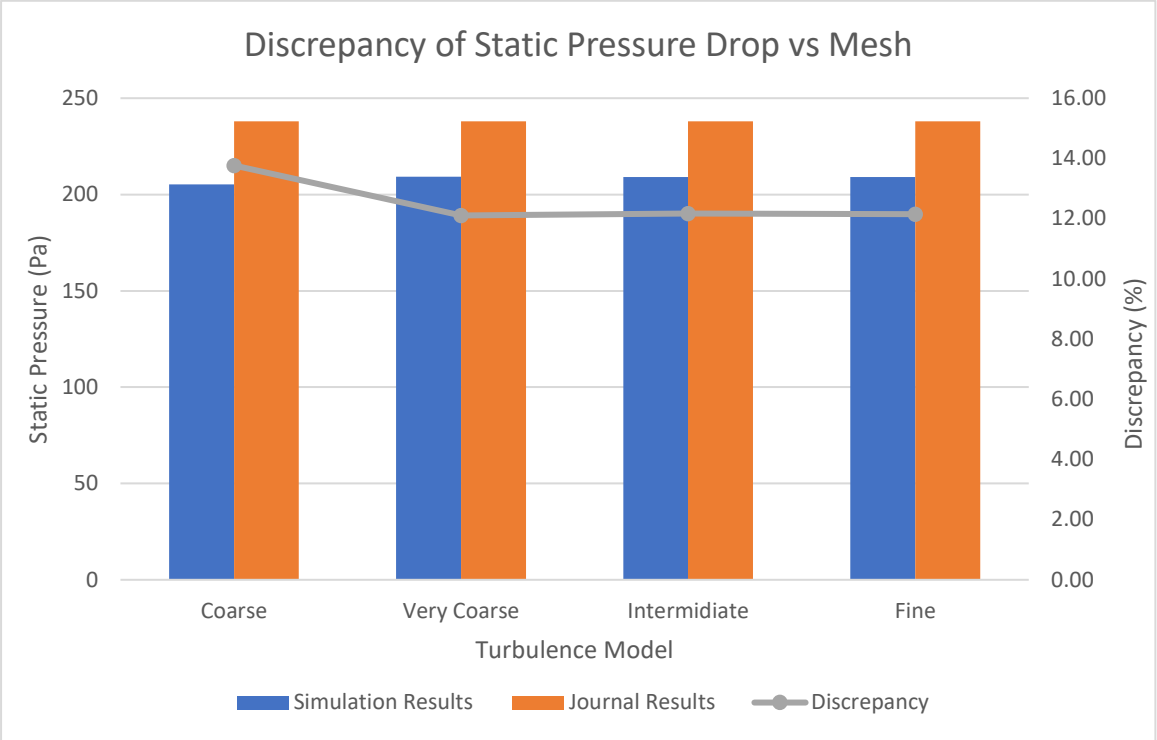

Figure 5: Comparison of Static Pressure Drop between Simulation Results with Journal Results in a function of Mesh

Discrepancy between simulation results with journal results for different mesh have been plotted in Figure 5. Discrepancy decreases dramatically from very coarse mesh to coarse mesh, which is 13.76% to 12.11%. However, the discrepancy does not change significantly from coarse mesh to fine mesh even though the mesh number increases histrionically. Table 7 shows the numerical results from Figure 5.

Since finer mesh does not reduce the discrepancy significantly from very coarse mesh and with the concern of computational power and time available, coarse mesh with 271,401 mesh number has been selected for the further validation and study.

Table 7: Tabulated Results from Figure 5

Mesh	Static Pressure Drop (Pa)		
	Simulation	Journal	Discrepancy
Very Coarse	205.24	238	13.76
Coarse	209.19		12.11
Intermediate	209.05		12.16
Fine	209.10		12.14

4.2. Turbulence Model Validation

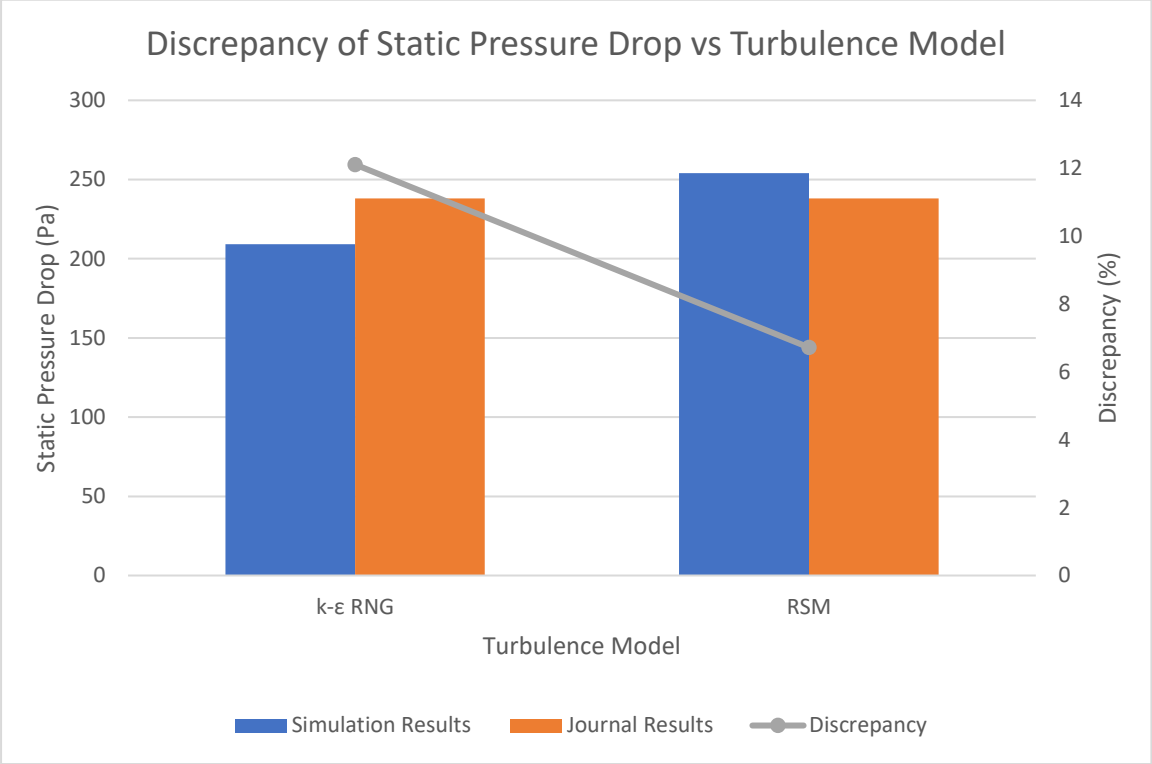

Figure 6: Results of Turbulence Model Validation between k-ε RNG and RSM Turbulence Model.

Coarse grid is used to run the simulation by using different turbulence model at the same inlet velocity, $9.95 ms^{-1}$.From Figure 6, k-ε RNG turbulence model gives 209.19Pa of static pressure drop, which is 12.11% discrepancy from the journal results which RSM turbulence model gives 254.02Pa of static pressure drop, which is 6.72% discrepancy from the journal results. Table 8 shows the numerical results from Figure 6.

In short, RSM turbulence model gives a better result with less discrepancy. Besides that, this achieve the conclusion from the journal (19), RSM turbulence model is more in reasonable

agreement with experimental data, compared with k-ε and k-ε RNG turbulence models. Hence, RSM turbulence model is used for the further validation and study.

Table 8: Tabulated Results from Figure 6

Turbulence Model	Static Pressure Drop		
	Simulation	Journal	Discrepancy
k-ε RNG	209.19	238	12.11
RSM	254.02		6.72

4.3. Simulation Results Validation

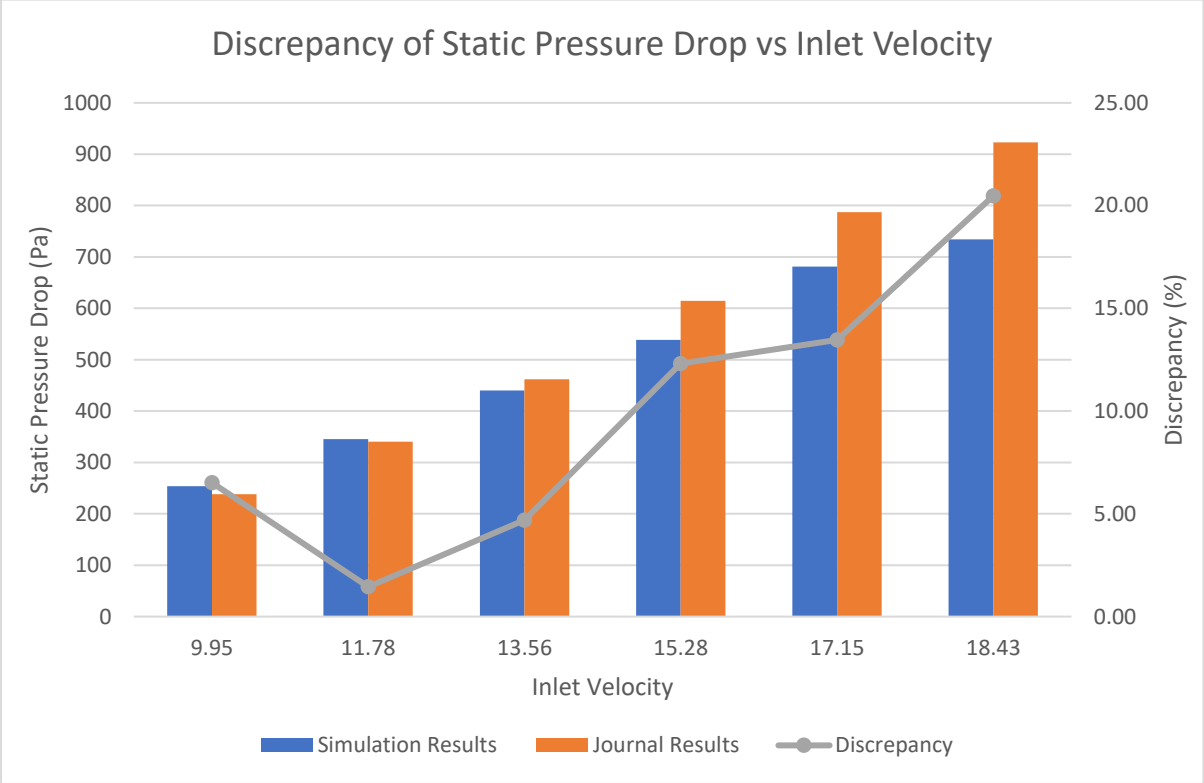

Figure 7: Comparison of Static Pressure Drop between Simulation Results with Journal Results in a function of Inlet Velocity.

Figure 7 shows the discrepancy of static pressure drop in a function of inlet velocity. Discrepancy decreases around 5.07% from 9.9 ms^{-1} to 11.78 ms^{-1}, then basically it shows a positive trend with increasing inlet velocity from 1.45% discrepancy at 11.78 ms^{-1} to 20.47% discrepancy at 18.43 ms^{-1}. Table 9 shows the numerical results from Figure 7.

Table 9: Tabulated Results from Figure 7.

Inlet Velocity (ms^{-1})	Static Pressure Drop (Pa)		
	Simulation	Journal	Discrepancy (%)
9.95	254	238.5	6.52
11.78	345.2	340.3	1.45
13.56	440.42	462.1	4.69
15.28	538.83	614.5	12.32
17.15	681.06	787.0	13.46
18.43	734.31	923.3	20.47

(17) concluded that no current Reynolds Average Navier-Stokes (RANS) turbulence model can predict the whole range of complex turbulent flows to worthwhile engineering accuracy. Besides that, RANS model will give approximately 15% discrepancy. In other words, this numerical model is considered as reliable because the discrepancy is within 15% for most cases even though the maximum percentage difference is 20.47% at inlet velocity of 18.43. In conclusion, robust numerical model has been developed and it will be used for further study in transient state.

4.4 Flow Pattern Identification in Transient State

Velocity magnitude is observed in contour plot and vector plot, shown in Figure 8. Horizontal cross-sectional plane shows the air flow in circulation following the cyclonic body of the cyclone. Besides that, the air velocity moves slower when it is near to the walls. Friction due to the effect of the air's viscosity near to the walls of cyclone separator slow the velocity nearby.

Vertical cross-sectional plane of vector plot shows the movement of air flow inside the cyclone. The air move in swirling pattern from the inlet to the cone tip. The air velocity decreases slowly along the swirling process and almost stationary when it reaches the cone tip. Sudden change in pressure allows the air move upward to the outlet. The velocity magnitude is shown in contour plot. Inlet velocity of $13ms^{-1}$, $16ms^{-1}$, and $22ms^{-1}$ have the same flow pattern inside while $7ms^{-1}$ has slightly different flow pattern. From the qualitative results, it has lower average air velocity. Inlet velocity of $7ms^{-1}$ might be out of the range for the working inlet